BIOCHEMISTRY
including biophysical chemistry & molecular biology

Article

pubs.acs.org/biochemistry

Surface Plasmon Resonance Analysis of the Binding Mechanism of Pharmacological and Peptidic Inhibitors to Human Somatic Angiotensin I-Converting Enzyme

Faïza Zidane,[§,‡] Gabrielle Zeder-Lutz,[†] Danièle Altschuh,[†] Jean-Michel Girardet,[§,‡] Laurent Miclo,[§,‡] Catherine Corbier,[§,‡] and Céline Cakir-Kiefer*[,§,‡]

[§]Université de Lorraine, Unité de Recherche Animal et Fonctionnalités des Produits Animaux (UR AFPA), Équipe Protéolyse et Biofonctionnalités des Protéines et des Peptides (PB2P), Faculté des Sciences et Technologies, Campus Aiguillettes, BP 70239, Vandœuvre-lès-Nancy F-54506, France

[‡]INRA, UR AFPA, Unité Sous Contrat 340, Vandœuvre-lès-Nancy F-54506, France

[†]Biotechnologie et signalisation cellulaire, Université de Strasbourg - CNRS, ESBS, Boulevard Sébastien Brant BP 10413, Illkirch F-67412, France

Supporting Information

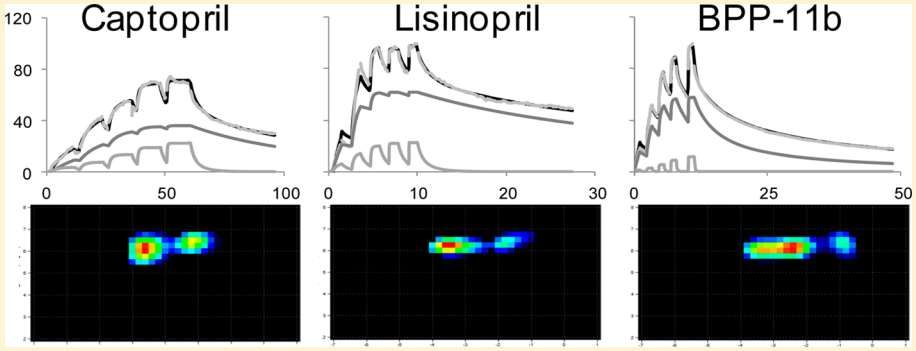

ABSTRACT: Somatic angiotensin I-converting enzyme (ACE) possesses two catalytic domains and plays a major role in the regulation of blood pressure, thus representing a therapeutic target for the treatment of hypertension. We present a comprehensive surface plasmon resonance (SPR) study of the interaction of human somatic ACE with the pharmacological inhibitors captopril and lisinopril, the bradykinin potentiating peptide BPP-11b, and the food peptidic inhibitors from bovine α_{s2}-casein, $F^{174}ALPQYLK^{181}$ and $F^{174}ALPQY^{179}$. SPR binding curves recorded with the high potency inhibitors captopril, lisinopril, and BPP-11b were evaluated both by regression analysis and by kinetic distribution analysis. The results indicated that captopril and lisinopril bound ACE with two K_D's differing by a factor 10−20 and >30, respectively (lowest K_D = 0.1−0.3 nM for both inhibitors). This shows, for the first time in a direct binding assay with the two-domain enzyme, the existence of two binding modes of the pharmacological inhibitors, presumably with the two ACE domains. The BPP-11b−ACE binding curves were complex but showed a predominant interaction with K_D in the nanomolar range. The caseinopeptides, known to inhibit ACE with an IC_{50} of 4.3 μM, bound to ACE with K_D = 3−4 μM. Mapping of the $F^{174}ALPQY^{179}$ binding site on ACE by sequential binding studies using captopril or BPP-11b indicated that it bound to (or near) the two active sites of ACE, in agreement with the stoichiometry of 2 determined from data fitting. Our results provide a detailed characterization of ACE-inhibitor binding modes and validate SPR for predicting the inhibitory potential of new compounds.

Somatic angiotensin I-converting enzyme (ACE; peptidyl-dipeptidase A, EC 3.4.15.1) is a zinc-metallopeptidase known to play a major role in the increase of blood pressure level. It converts angiotensin I, an inactive decapeptide, to angiotensin II, a powerful vasoconstrictor. Moreover, ACE catalyzes the degradation of bradykinin, a nonapeptide involved in vasodilatation.

Somatic ACE is a membrane-anchored enzyme chiefly located in endothelial, epithelial, and neuronal cells and consists of two homologous amino and carboxyl domains (55% amino acid sequence identity), each domain possessing its own catalytic site with the zinc-binding motif HEMGH.[1]

Considering the crucial role of somatic ACE in the regulation of blood pressure, this enzyme is a key therapeutic target for the treatment of hypertension, which represents a risk factor in the development of cardiovascular and kidney diseases. The search

Received: May 15, 2013
Revised: October 28, 2013
Published: October 29, 2013

for preventive or therapeutic treatments is an important worldwide public-health challenge. The first ACE inhibitors highlighted are bradykinin potentiating peptides (BPPs) isolated from *Bothrops jararaca* venom.[2] These peptides show a strong ACE inhibitory activity (nanomolar K_i) *in vitro*[3] and *in vivo* when administrated intravenously in Wistar rats and Swiss mice.[4] However, BPPs lose their effectiveness by the oral route, which can explain why they are not used as drugs to treat hypertension.[5] Captopril, the first commercial ACE inhibitor orally active, is used as an antihypertensive drug.[6] Currently, many other synthetic ACE inhibitors, such as enalapril and lisinopril, are available for clinical uses.[7] However, their chronic administration to treat hypertension may generate some side effects, such as dry coughing and angioedema.[5]

ACE-inhibitory peptides generated by hydrolysis of various food proteins, particularly milk proteins,[8] may provide a natural and safe alternative to prevent hypertension. Indeed, no known side effect is associated with their consumption to date,[9] and although they are less efficient than synthetic inhibitors, they could be effective in maintaining a healthy level of blood pressure. A previous study carried out in our lab on the inhibitory potency of peptides released by trypsin from bovine α_{s2}-casein has highlighted the presence of eight ACE-inhibitory peptides, the most efficient being F^{174}ALPQYLK^{181} and F^{174}ALPQY^{179} with an identical IC_{50} of 4.3 μM.[10]

Several methods have been used to assess the ACE-inhibitory potency of peptidic or pharmacological inhibitors. Most *in vitro* tests are based on the enzymatic method of Cushman and Cheung[11] by quantifying an hydrolysis product in the presence or in the absence of a given inhibitor using reversed-phase HPLC.[10] Other methods have been also employed, but to a lesser extent, such as fluorescence resonance energy transfer[12] and isothermal titration calorimetry.[13] These methods have, however, the disadvantage of being indirect, not very sensitive, and time-consuming and/or requiring a large quantity of ACE. Although a quartz crystal microbalance (35 mHz) and an AutoLab surface plasmon resonance (SPR) have been used to investigate the lisinopril-ACE binding,[14] the real-time information on the interaction between ACE and its inhibitors is still limited. To our knowledge, the Biacore SPR technology has never been used to study the interaction between ACE and inhibitory peptides or pharmacological molecules. Its ability to monitor association and dissociation kinetics for molecular interactions provides detailed information on the mechanism of complex formation, together with the affinity and stoichiometry of the interaction.[15] Moreover, this technology does not require a large amount of enzyme in an experimental setup where binders are flown over the surface-immobilized enzyme.

Our objective was to use a direct label-free approach, SPR-based biosensing (Biacore), to determine the drug target ACE binding properties of different specific inhibitors, in order to derive kinetic and affinity parameters and map the binding sites. To this end, we chose three types of inhibitors: (i) the pharmacological inhibitors captopril and lisinopril, which inhibit competitively both the amino and carboxyl active sites of ACE,[16,17] (ii) the bradykinin potentiating peptide BPP-11b (<EGLPPRPKIPP, where <E corresponds to a pyroglutamyl residue) which is highly selective for the carboxyl domain,[18] and (iii) the food peptidic inhibitors from bovine α_{s2}-casein, F^{174}ALPQYLK^{181}, and F^{174}ALPQY^{179}.[10] Because of their different inhibitory behaviors toward the somatic ACE, captopril and BPP-11b were used in a SPR competition assay in order to determine if the inhibitory peptide FALPQY binds to the amino active site of ACE or the carboxyl active site, or both.

EXPERIMENTAL PROCEDURES

CHO-ACE Cell Culture and Membrane-Bound ACE Recovery. Adherent Chinese hamster ovary cell line transfected with a full-length cDNA encoding human somatic ACE and expressing high levels of membrane-bound wild-type ACE (called here CHO-ACE) was established by Wei et al.[19] and kindly supplied by Prof. François Alhenc-Gelas from the Institut National de la Santé et de la Recherche Médicale (INSERM, Paris, France).

CHO-ACE cells were cultured in flasks T150 (BD Biosciences, Le Pont-de-Claix, France) at 37 °C in the presence of air enriched with 5% CO_2 in Ham's F-12/Dulbecco's modified Eagle's medium (Life Technologies SAS, Saint-Aubin, France) containing 15 mM Hepes and phenol red. This medium was supplemented with 10% fetal calf serum (Sigma-Aldrich Co., St-Quentin-Fallavier, France) heated at 56 °C for 30 min, 750 μg/mL Geneticin (Life Technologies SAS) and 4 mM L-glutamine (Sigma-Aldrich Co.).

At confluence, culture medium was removed from flasks, and cells were washed three times with PBS buffer to eliminate bovine ACE contained in fetal calf serum and then fed again with a serum-free medium supplemented with 80 μM $ZnSO_4$. After a 48-h incubation, culture medium was removed from flasks, and adherent cells were incubated for 15 min with an ice-cold PBS and removed from flasks by scraping. In order to eliminate PBS, cells suspension was centrifuged at 3320*g* at 4 °C for 15 min. The pellet was recovered and resuspended in 10 mM Hepes buffer, pH 8, containing 100 mM NaCl, 1 mM $CaCl_2$, and 1 μM $ZnSO_4$. This operation was repeated three times, and then cells were suspended in the Hepes buffer.

Membrane-bound ACE was released from CHO-ACE cells by L-1-tosylamide-2-phenylethyl chloromethyl ketone-treated trypsin (EC 3.4.21.4) from bovine pancreas (Sigma-Aldrich Co.). For this purpose, the CHO-ACE cell suspension was incubated for 1 h at 37 °C with 10 mg trypsin/g total protein. The pH was then adjusted at 5.2 with 1.75 M acetic acid, and the cell suspension was gently stirred for 30 min at 4 °C. Straight afterward, the suspension was centrifuged for 30 min at 20000*g* and 4 °C. The pH values of the solution of pellet resuspended in the Hepes buffer and of the supernatant were adjusted to 8.0 and 8.3, respectively, with 0.4 M NaOH. They were then reincubated for 30 min at 37 °C. The supernatant was kept on ice, while the pellet was submitted to a second trypsinolysis under the same conditions. Newly generated supernatant was pooled with the previous one, and the solution was concentrated by centrifugation with a 100-kDa molecular mass cutoff membrane (Merck Millipore, Billerica, MA, USA) at 4 °C before being stored at −20 °C.

ACE Activity Assay. ACE enzymatic activity was determined by quantifying hippuric acid released by hydrolysis of the synthetic substrate hippuryl-L-His-L-Leu (HHL) using reversed-phase HPLC according to a method adapted from that of Tauzin et al.[10] Briefly, a volume of 20 μL of enzymatic solution was added to 130 μL of 50 mM Hepes buffer, pH 8.3, containing 5.2 mM HHL and 300 mM NaCl and incubated at 37 °C for 5−60 min. The enzymatic reaction was then stopped by adding 75 μL of inhibiting solution composed of 15 μM captopril (Sigma-Aldrich Co.), 3 mM trisodium EDTA, and 0.2% (v/v) trifluoroacetic acid. The hippuric acid quantification was performed according to Tauzin et al.[10] Increasing

dx.doi.org/10.1021/bi4006144 | *Biochemistry* 2013, 52, 8722−8731

quantities of hippuric acid were injected on the C_{18} column in order to plot a standard curve and calculate enzyme activity. One unit of ACE activity corresponds to 1 μmol of hippuric acid produced per min.

ACE Purification by Affinity Chromatography and Characterization. Purification of recombinant somatic ACE was carried out on lisinopril Sepharose 6B column (GE Healthcare, Uppsala, Sweden) according to a method adapted from that of Bull et al.[20] The solution containing the trypsin-solubilized form of ACE was concentrated and washed 10 times with 15 mM Hepes buffer, pH 8.3, containing 250 mM NaCl and 10 μM $ZnSO_4$ by centrifugation at 3320*g* at 4 °C using Amicon concentrators with a 100-kDa cutoff membrane (Merck Millipore). Afterward, the solution was centrifuged for 15 min at 3320*g* at 4 °C, and its pH (which should be close to 8.3) and absorbance at 280 nm were measured before loading the sample on the lisinopril Sepharose 6B column (3.1 × 1.0 cm) equilibrated with the Hepes buffer at 4 °C and at a flow rate of 0.8 mL/min. During the run, aliquots of 1 mL were collected and monitored at 280 nm. After removal of the unbound material by washing the column with Hepes buffer, elution of recombinant ACE was performed with the same buffer containing 10 μM lisinopril. These elution fractions were pooled and dialyzed at 4 °C against lisinopril-free Hepes buffer.

Apparent molecular mass and purity control of recombinant somatic ACE were determined by SDS−PAGE with a 5% (w/v) acrylamide stacking gel at pH 6.8 and a 7.5% (w/v) acrylamide resolving gel at pH 8.8 according to the method of Laemmli[21] with the Mini-Protean 3 system (Bio-Rad Laboratories Inc., Marnes-la-Coquette, France). The conditions of migration were 200 V, 500 mA, and 4 °C. After a 30−45 min migration, the proteins were revealed in gel by silver staining. Precision Plus Protein prestained standards (Bio-Rad) were used to provide a ladder of molecular masses.

Purification of Inhibitory Peptides. Peptides FALPQYLK and FALPQY were synthesized by PolyPeptide Group (Strasbourg, France), while peptide BPP-11b was obtained from Genosphere Biotechnologies (Paris, France). All these synthetic peptides were purified by reversed-phase HPLC as described by Zidane et al.[22] with a linear gradient 10−50% (v/v) acetonitrile in water and in the presence of 0.1% (v/v) trifluoroacetic acid for 80 min. Volumes of 500 μL of each peptide solution at 0.5 mg/mL were injected onto the column per run. Pure peptides were collected, freeze-dried, and stored at −20 °C.

Determination of Protein and Peptide Contents. Total protein content was determined according to the method of Bradford[23] using bovine serum albumin as standard. Measurements were performed in triplicates. The ACE concentration was determined by measuring its absorbance at 280 nm and using its theoretical molar extinction coefficient of 309815 M^{-1} cm^{-1} calculated with ProtParam tool available online (http://web.expasy.org/protparam/).

Peptide concentrations were determined by quantifying free amino groups of peptides by the *o*-phthaldialdehyde method of Frister et al.[24] at 340 nm with an MRX microplate reader (ThermoLabsystems, Chantilly, VA, USA). Measurements were carried out in triplicates. The presence of reactive ε-amino group (in peptides containing lysyl residues) or the absence of α-amino group in BPP-11b (pyroglutamyl residue at amino-terminus position) was taken into account.

SPR Analysis of ACE−Inhibitor Interactions. The interaction studies were carried out in real time by SPR analysis using a Biacore 2000 or Biacore T200 instrument (GE Healthcare Biacore). A carboxymethylated dextran sensor chip CM5 (BR-1000-12, GE Healthcare Biacore) was used to immobilize the purified enzyme via the standard amine coupling method.

All experiments were carried out at 25 °C. A filtered (0.22 μm) and degassed mixture of 10 mM Hepes, pH 7.4, containing 150 mM NaCl, 1 μM $ZnSO_4$ and 0.005% (v/v) Tween 20 was used as running buffer for the immobilization and stabilization of ACE. The four flow cells (FC) of a CM5 sensor surface were activated with a 1:1 (v/v) mixture of 0.2 M *N*-ethyl-*N*′-(3-dimethylaminopropyl)-carbodiimide hydrochloride and 0.05 M *N*-hydroxysuccinimide for 10 min (5 μL/min). Various quantities of ACE that had been dialyzed at 4 °C in 10 mM sodium acetate buffer, pH 4.0, were immobilized on two FC by injection of a 0.26-μM solution at a flow rate of 5 μL/min. The response levels were in the range of 4150−8770 and 9960−11790 resonance unit (RU) for FC1 and FC2, respectively. As a negative control, bovine α_{s1}-casein purified according to Miclo et al.[25] was dissolved at 1 mg/mL in 10 mM sodium acetate buffer, pH 4.0, and immobilized on FC3. FC4 contained no ligand and served as a reference. Remaining reactive groups on the matrix were blocked by treatment with 1 M ethanolamine adjusted to pH 8.5 with HCl.

For binding experiments, filtered and degassed 10 mM Hepes buffer, pH 7.4, containing 300 mM NaCl, 1 μM $ZnSO_4$, and 0.005% (v/v) Tween 20 (HBS-B) was used as dilution and running buffer for binding experiments. Serial dilutions of each purified peptide were injected over the four cells at a flow rate of 30 μL/min (MCK, multicycle kinetics). Each cycle consisted of a 60-s sample injection (except for BPP-11b: 600 s) followed by a postinjection phase of 500 s for FALPQYLK and FALPQY, and of 6000 s for BPP-11b. Captopril, lisinopril, and BPP-11b were analyzed using single-cycle kinetic (SCK) runs with successive 60 or 600 s injections of the samples followed by a single postinjection phase of at least 20 min. The tripeptide GGG (Sigma-Aldrich Co.) at a concentration of 50 μM was used as negative control. Captopril and lisinopril were also used to evaluate the binding capacity of the immobilized ACE.

The binding curves were prepared by double referencing, that is, subtraction of the sensorgram recorded on the reference flow cell (FC4), followed by subtraction of a sensorgram resulting from HBS-B buffer injection on the ACE surface. Data were XY-zeroed and the resulting binding curves were analyzed by regression analysis, using the softwares BIAevaluation T200 version 1.0 (GE Healthcare), BIAevaluation 2000 version 3.0 (GE Healthcare), or Scrubber 2.0c (BioLogic Software, Campbell, Australia). The association (k_{on}) and dissociation (k_{off}) rate constants, the equilibrium dissociation constant ($K_D = k_{off}/k_{on}$), the maximum response *R*max, and the binding stoichiometry (n) were determined using the heterogeneous ligand model with two parallel interactions or the Langmuir binding model. The theoretical binding capacity ($Rmax_{theor}$) of the surface was calculated from the level of fixed ACE (RU_{ACE}), and M_r of ACE ($M_{r\,ACE}$) and inhibitors ($M_{r\,inhibitor}$), as

$$Rmax_{theor} = RU_{ACE} M_{r\,inhibitor}/M_{r\,ACE} \quad (1)$$

assuming a one ACE/one inhibitor stoichiometry. The experimental binding capacity of the surface (*R*max) was fitted from kinetic or affinity data evaluation. The binding stoichiometry (n) was calculated as the ratio of fitted to theoretical binding capacity:

dx.doi.org/10.1021/bi4006144 | *Biochemistry* 2013, 52, 8722−8731

$$n = R\max / R\max_{\text{theor}} \quad (2)$$

The binding curves (for captopril, lisinopril, and BPP-11b) were also interpreted from kinetic distribution analysis using the tool Interaction Map (Ridgeview Diagnostics, Uppsala, Sweden). The software decomposes the curves into the contributions of parallel interactions and presents the results as an interaction map (k_{off} on the x-axis; k_{on} on the y-axis), where each peak represents an interaction event.

The sequential binding studies were performed with FALPQY and captopril or with FALPQY and BPP-11b. An injection of the running buffer HBS-B or of a 200-nM captopril solution (120 s; 10 μL/min) or a 9-nM BPP-11b solution (600 s; 10 μL/min) was followed by an injection of either running buffer or 30 μM FALPQY (90 s; 10 μL/min) and a 7000-s postinjection phase. The Scrubber 2.0c software was used for data analysis.

RESULTS

ACE Expression, Purification, and Characterization. Human recombinant somatic ACE expressed in CHO-ACE cell line was solubilized from cell membranes by trypsin which removed its membrane anchor without altering its catalytic activity.[26] After purification, ACE was recovered with high degree of purity upper to 90% and displayed an apparent molecular mass of ca. 187 kDa (Figure 1) and a specific activity toward HHL of 26.8 U/mg of protein, close to the specific activity of 24 U/mg determined by Nishimura et al.[27]

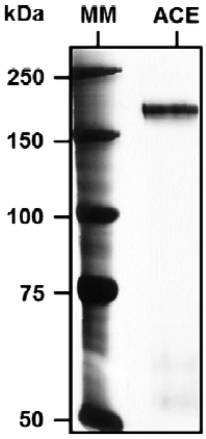

Figure 1. Purity control of ACE. The SDS-PAGE profile using 7.5% (v/v) acrylamide resolving gel shows the purified recombinant human somatic ACE expressed in CHO-ACE cell line solubilized by trypsin and stained by silver nitrate. MM: molecular mass standards.

Assessment of the Binding Capacity of Immobilized ACE. The well-known pharmacological ACE inhibitors captopril (an *N*-thioalkyl derivative of the dipeptide sequence AP) and lisinopril (tripeptide analogue of FKP) were used as reference analytes to estimate the binding capacity of ACE when covalently immobilized on sensor surfaces. Indeed, the standard amine coupling of proteins results in random immobilization, with different orientations that lead to a partial steric hindrance of the binding sites.[28] On the other hand, a partial ACE denaturation might occur during the successive experimental steps such as freezing, defrosting, dialysis, and immobilization. The SPR response expected at surface saturation ($R\max_{\text{theor}}$) can be calculated knowing that the enzyme possesses two active sites, each being able to recognize and bind an inhibitor molecule.[13,14,17,29] The experimental maximal response (Rmax) was obtained by injecting samples containing increasing concentrations of the inhibitors over the ACE surfaces. The fraction of functional ACE is given by the ratio of observed to expected saturation response.

The SPR binding curves corresponding to the injection of captopril or lisinopril over two surfaces with different ACE densities are shown in Figure 2, panels A and B, respectively. Surface saturation was clearly achieved in the case of lisinopril, with observed responses of 26 and 10 RU on the two ACE surfaces (Figure 2B). The calculated saturation responses were 52 and 22 RU, respectively. Consequently, the fraction of functional ACE is ca. 50% (26/52 or 10/22). Surface saturation is almost reached in the case of captopril with experimental responses around 12 and 10 RU (Figure 2A), as compared to calculated saturation responses of 30 and 22 RU, respectively, confirming that the fraction of functional enzyme lies around 50%. This value will be used to correct experimental stoichiometries thereafter.

Binding of Captopril or Lisinopril to Immobilized ACE. The binding curves showing the real-time association and dissociation of captopril and lisinopril onto immobilized ACE were analyzed by regression analysis using either the 1:1 Langmuir binding model or the heterogeneous ligand model, which describes the different interactions of the analyte with two different immobilized binding sites.

The two interactions were difficult to describe with high precision because the SPR signal was small due to the low molecular weight of the inhibitors and because binding was limited by mass transport (data not shown). Reducing the amount of immobilized ACE to prevent mass transport was not possible because the SPR signal would then be reduced as well.

The fits were better in the case of the heterogeneous ligand model (Figure 2A,B), with an average Chi2 < 0.26, as compared to >0.7 obtained with the Langmuir model. In the case of captopril, the fits indicated the existence of two interactions with K_D around 0.1 and 1.3 nM (Table 1). The corrected stoichiometries were similar (0.84, 0.80; Table 1) as expected if the two interactions correspond to the binding of captopril to the two ACE active sites. The half-time $t_{1/2}$ of the strong and weak affinity complexes, calculated from the off-rate constants, were ~1 h and 2.2 min, respectively.

Regression analysis of the ACE−lisinopril binding curves indicated two interactions with K_D's around 0.1 and 2.4 nM (Table 1). The corrected stoichiometries were 1.3 and 0.7 lisinopril/ACE for the strong and weak interactions, respectively. The half-time $t_{1/2}$ of the strong and weak affinity complexes, calculated from the off-rate constants, were ~1.3 h and 2.3 min, respectively.

Interaction Study between Immobilized ACE and the Selective Peptide Inhibitor BPP-11b. Binding kinetics of BPP-11b to ACE were investigated in SCK runs by injecting concentrations of BPP-11b ranging from 1.9 to 150 nM. When fitting the data to the 1:1 Langmuir binding model (Figure 2C), BPP-11b was found to bind to ACE with K_D = 0.51 nM and a corrected stoichiometry of ≈1 (Table 1), suggesting the presence of a predominant BPP-11b binding site on ACE. These results are in accordance with the findings of Cotton et al. who showed that this peptide bound preferentially to the carboxyl domain (apparent K_i = 30 nM) of human somatic ACE, and with a 266-fold weaker affinity to the amino domain (apparent K_i = 8000 nM).[18]

dx.doi.org/10.1021/bi4006144 | *Biochemistry* 2013, 52, 8722−8731

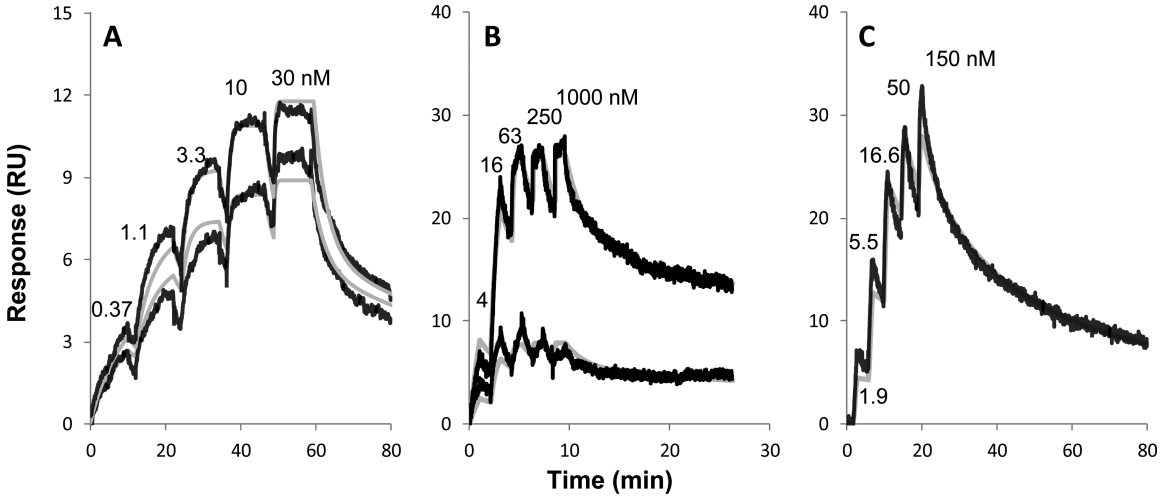

Figure 2. Regression analysis of the SCK binding curves recorded for the ACE−inhibitor interactions. (A) Increasing concentrations of captopril (0.37−30 nM) were injected successively over two surfaces with immobilized recombinant human somatic ACE (8770 and 11790 RU). (B) Increasing concentrations of lisinopril (4−1000 nM) were injected simultaneously over two surfaces with immobilized ACE (4150 and 10000 RU). (C) BBP-11b at concentrations ranging between 1.9 and 150 nM was injected over a surface with immobilized ACE (9960 RU). The sample injections lasted for 10 min (A) or 1 min (B and C), and were separated by a 2-min buffer wash. The experimental curves (black) were fitted to the heterogeneous ligand binding model with two parallel interactions (A and B) or the 1:1 Langmuir binding model (C) using the BIAevaluation T200 software (version 1.0). Fitted curves are in gray.

Table 1. Kinetic and Equilibrium Constants for the Interaction of Captopril, Lisinopril, and BPP-11b with the Immobilized ACE[a]

		k_{on} (10^6 M^{-1} s^{-1})	k_{off} (10^{-3} s^{-1})	K_D (nM)	experimental stoichiometry (mol/mol ACE)	corrected stoichiometry[d] (mol/mol ACE)
captopril[b]	Site 1	1.4 ± 0.8	0.17 ± 0.05	0.15 ± 0.09	0.42 ± 0.05	0.84 ± 0.1
	Site 2	8.6 ± 6.0	5.1 ± 0.7	1.3 ± 1.4	0.40 ± 0.05	0.80 ± 0.1
lisinopril[b]	Site 1	1.3 ± 0.4	0.14 ± 0.14	0.10 ± 0.08	0.67 ± 0.02	1.34 ± 0.04
	Site 2	1.8 ± 0.6	4.9 ± 4.9	2.4 ± 1.9	0.33 ± 0.02	0.66 ± 0.04
BPP-11b[c]		1.2 ± 0.6	0.65 ± 0.31	0.51 ± 0.34	0.43 ± 0.08	0.86 ± 0.16

[a]Standard error values were calculated from four to five measurements for each analyte. [b]Data were fitted with the heterogeneous ligand model (two parallel interactions). [c]Data were fitted with the 1:1 Langmuir binding model. [d]Values corrected according to functional ACE percentage (*ca.* 50%).

Kinetic Distribution Analysis of the Binding Data of Captopril, Lisinopril, and BPP-11b. Regression analysis of kinetic data is limited to relatively simple binding models and can provide acceptable fits even when the model does not conform to the complexity of experimental data. Alternative mathematical approaches have been proposed that decompose kinetic curves into the contributions of parallel interactions, based on a two-dimensional distribution of kinetic parameters.[30−33] In contrast with regression analysis, kinetic distribution analysis of kinetic curves does not require *a priori* assumptions regarding the number of interactions contributing to the curve. We have used Interaction Map (Ridgeview Diagnostics) to investigate if the kinetic curves recorded with captopril and lisinopril indeed conform to the sum of two parallel interactions, and to further investigate the complexity of the ACE−BPP-11b interaction. The maps calculated from three different ACE−captopril, ACE−lisinopril, or ACE−BPP-11b kinetic curves are shown in Figure 3.

The kinetic distribution analysis of the curves recorded with captopril and lisinopril identified two peaks, indicating the contribution of two interactions to the curves (Figure S1, Supporting Information). The kinetic/affinity parameters of the weakest interactions were difficult to resolve precisely because of their small contribution to the SPR signal at low inhibitor concentration. Furthermore the signal itself was small (<26 RU at surface saturation) because of the low M_r of the inhibitors. Despite these technical challenges, the peak patterns obtained in three independent experiments were strikingly similar. The peaks were located on a same level in the *y*-direction indicating similar on-rate constants and were separate in the *x*-direction indicating different off-rate constants and therefore equilibrium affinity constants. The two peaks in the ACE−lisinopril maps (Figure 3D−F) consistently lay further apart than those in the ACE−captopril maps (Figure 3A−C), indicating a larger difference in affinity between the two interactions contributing to the ACE−lisinopril curves compared to those contributing to the ACE−captopril curves. The most stable interaction, in both the lisinopril and captopril maps, showed a K_D in the 0.1−0.3 nM range. The weakest interaction showed a K_D in the 2−4 nM range in the case of captopril and >8 nM in the case of lisinopril. These values are consistent with those found from regression analysis (Table 1), except for the lower affinity (>8 nM) of the weakest ACE−lisinopril interaction. The decomposition of each kinetic curve into the two contributing interactions is shown in Figure S1, Supporting Information.

The peak weights reflect their contribution to the overall signal. They are expected to be higher for the strongest compared to the weaker interaction if surface saturation was not reached. The highest affinity peak contributed between 45 and 65% of the signal, while the lowest affinity peak contributed

dx.doi.org/10.1021/bi4006144 | *Biochemistry* 2013, 52, 8722−8731

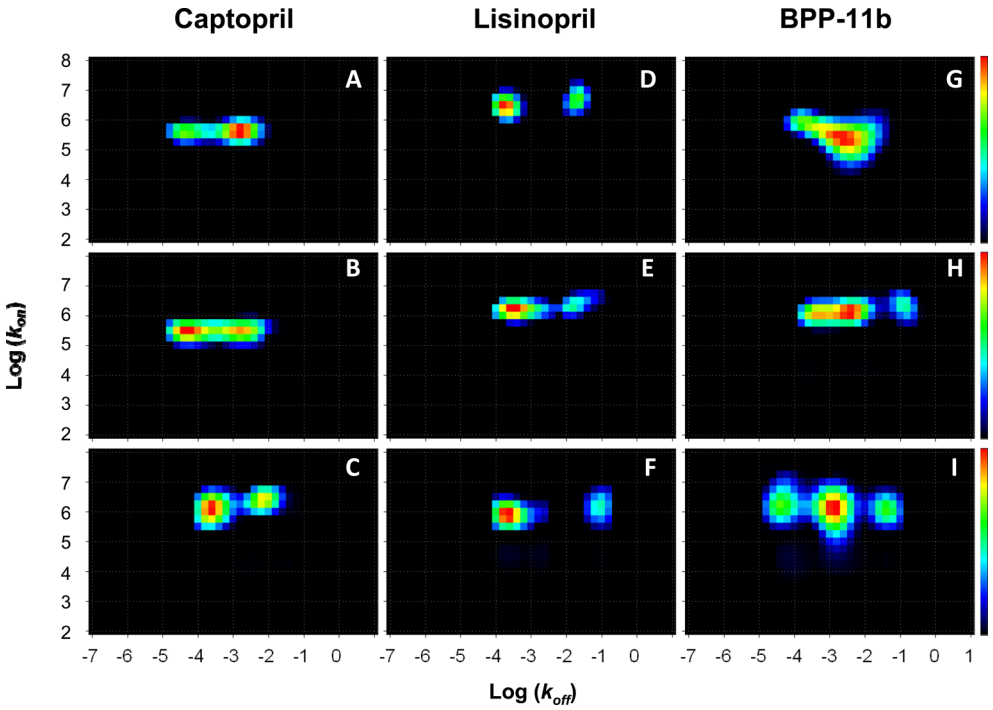

Figure 3. Kinetic distribution analysis of the SCK binding curves recorded for the ACE−inhibitor interactions. Three SCK binding curves recorded for captopril (A, B, C), lisinopril (D, E, F), and BPP11b (G, H, I) were evaluated with the Interaction Map software. The maps display each interaction contributing to the measured binding curve as a peak using log (k_{on}) and log (k_{off}) coordinates. Colors represent the relative degree of contribution of the different interactions (red: large contribution, blue: small contribution). The inhibitor concentrations were 2.5−200 nM (A and B) and 0.4−30 nM (C) for captopril, 4−1000 nM (D and E) and 3.7−300 nM (F) for lisinopril, 0.009−18 nM (G) and 1.85−150 nM (H and I) for BPP-11b. Recombinant human somatic ACE immobilization levels were from top to bottom 6575, 9960, and 11787 RU for assays with captopril, 4150, 10000, and 11790 RU for assays with lisinopril; 8080, 11790, and 9960 RU for assays with BPP-11b. The decomposition of the experimental curves into the contributing interactions is shown in Figure S1, Supporting Information.

to 22 and 45% of the signal. The weight parameter is difficult to determine precisely, in particular when one high affinity interaction is compared to a low affinity interaction and the concentrations used do not fully saturate the lower-affinity binding site. Under such conditions, the weight may be less precise and its value of indicative nature.

We also verified that simulated mass transport-influenced kinetic curves produce a single peak (data not shown). The two peaks identified from the ACE−lisinopril and ACE−captopril kinetic curves are therefore not related to mass transport.

The kinetic distribution analysis of the ACE interaction with BPP-11b produced complex maps (Figure 3G−I). The predominant peak corresponded to an interaction with nanomolar affinity, consistent with the global K_D calculated from regression analysis using the Langmuir model. The peak is broadened toward higher affinities (slower dissociation) in two of three experiments (Figure 3G,H) and a higher affinity peak appears in the last one (Figure 3I). The meaning of this pattern is unclear, but the existence of a different, stronger-affinity binding site can be excluded because it would be most populated (highest peak weight). A low affinity peak is present in all maps. These curves present complexities that could not be unraveled with the current approaches, possibly resulting from peptide BPP-11b conformational heterogeneity.

Interaction Study between Immobilized ACE and Inhibitory α_{s2}-Caseinopeptides. Sensorgrams of the interaction of ACE with FALPQYLK and FALPQY displayed similar profiles characterized by a fast dissociation of the ACE−peptide interactions (Figure 4A,B). Fits of the binding curves to the 1:1 Langmuir model indicated equilibrium dissociation constants of 3.1 μM for FALPQYLK and 3.7 μM for FALPQY (K_D, Table 2). These ACE−peptide affinities are weak when compared to those measured with captopril, lisinopril and BPP-11b, and close to the published IC_{50} value (4.3 μM[10]). Their similarity indicates that the carboxyl terminal dipeptide LK had no influence on the ACE binding properties as evaluated by Biacore SPR, consistent with their similar inhibitory capacity.[10] A corrected binding stoichiometry around 2 was calculated for both peptides, suggesting the existence of two peptide binding sites on ACE.

Development of a Mapping Method for the Determination of ACE−FALPQY Binding Sites. We used sequential binding experiments to determine if FALPQY bound either specifically to the active sites of ACE or to other surface regions of the enzyme. The peptide FALPQY was first studied in competition with captopril toward ACE. Hence, the binding sites of the amino and carboxyl domains of ACE were almost fully saturated by injection of a 200-nM captopril sample (ca. 200-fold the highest K_D). A solution of FALPQY at a concentration of 30 μM (ca. 8-fold the K_D value) was then injected and a remaining response signal of 2.7 RU was measured (Figure 5A), as compared to 19 RU in the absence of captopril (Figure 5B). Comparison between response signals of FALPQY in the presence and in the absence of captopril showed a signal loss of ca. 90%. The observation that the binding of FALPQY was almost fully blocked when ACE was saturated with captopril indicated that FALPQY bound at the same locations as captopril, presumably in or near the two active sites located on the two domains of ACE.

dx.doi.org/10.1021/bi4006144 | Biochemistry 2013, 52, 8722−8731

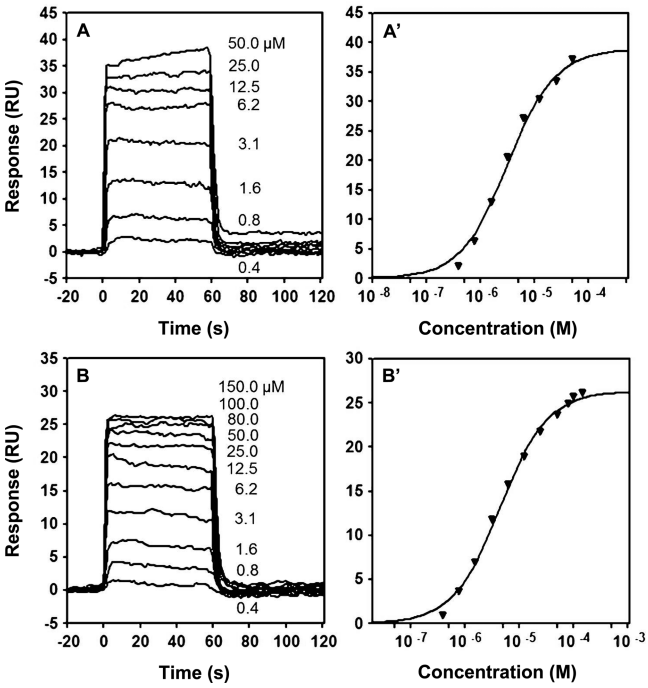

Figure 4. Analysis of the ACE−caseinopeptide interactions. Sensorgrams recorded when injecting samples with increasing concentrations of FALPQYLK (A) and FALPQY (B) over immobilized recombinant human somatic ACE (7860 RU) in MCK runs. Each cycle consisted of a 60-s sample injection followed by a postinjection phase of 500 s. Equilibrium responses were plotted as a function of FALPQYLK (A′) and FALPQY (B′) concentration and fitted to the 1:1 Langmuir binding model using Scrubber 2.0c software. The resulting equilibrium dissociation constants are reported in Table 2.

Table 2. Equilibrium Constants for the Interaction of the Peptide Inhibitors FALPQYLK and FALPQY with the Immobilized ACE[a]

	K_D (µM)	experimental stoichiometry (mol/mol ACE)	corrected stoichiometry[b] (mol/mol ACE)
FALPQYLK	3.1 ± 0.1	0.9 ± 0.1	1.8 ± 0.2
FALPQY	3.7 ± 0.1	0.9 ± 0.1	1.8 ± 0.2

[a]Data were fitted with the 1:1 Langmuir binding model using Scrubber 2.0c software. Standard error values were calculated from two measurements for each analyte. [b]Values corrected according to functional ACE percentage (*ca.* 50%).

In contrast to captopril, BPP-11b should only partially block FALPQY binding. Indeed BPP-11b is believed to bind preferentially to the carboxyl terminal domain of ACE,[18] as supported by the corrected stoichiometry close to 1 measured here (Table 1), while a stoichiometry of 2 was calculated for FALPQY (Table 2). In the present study, a concentration of 9 nM BPP-11b was used to investigate the competition between the latter and FALPQY toward ACE. At 9 nM, the preferential binding site of BPP-11b on ACE is predicted to be ca. 80% saturated (n = 0.8). If two FALPQY molecules are able to interact with one ACE molecule, and if one of the two binding sites is ca. 80% saturated with the BPP-11b thus leaving 1.2/2 (60%) sites available for FALPQY binding, we expect that the FALPQY response in the presence of BPP-11b will be ca. 60% of that in the absence of BPP-11b. The measured FALPQY responses in the presence and absence of BPP-11b were 14 and 25 RU, respectively (Figure 6A,B). The 56% FALPQY response remaining in the presence of BPP-11b was close to the expected response of 60%.

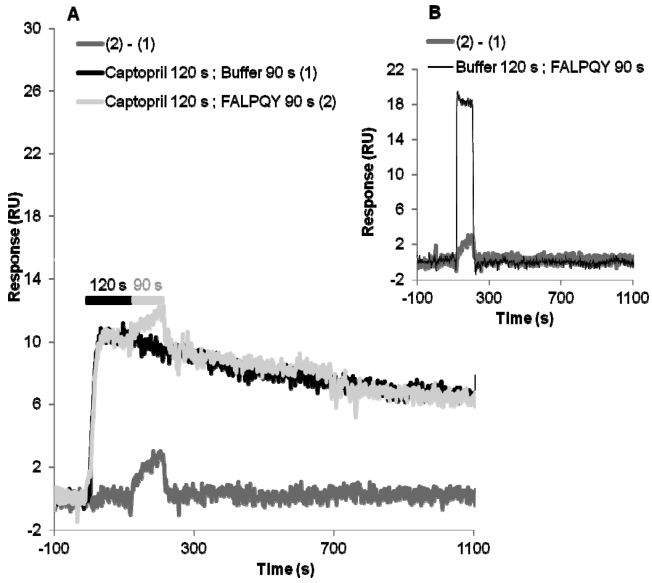

Figure 5. Competition between FALPQY and captopril for binding to immobilized recombinant human somatic ACE (7860 RU). (A) Injection of a saturating concentration of captopril (200 nM) for 120 s followed by a 90-s injection of either running buffer (1), or a saturating concentration of FALPQY (30 µM) (2). The signal remaining after subtracting (1) from (2) corresponds to the interaction of FALPQY with the captopril-saturated enzyme. (B) Comparison of this remaining (2) − (1) signal with that produced when FALPQY (30 µM) is injected in the absence of captopril.

DISCUSSION

We have applied the Biacore SPR technology to study the mode of binding of ACE with the pharmacological inhibitors captopril and lisinopril, with BPP-11b (a carboxyl domain selective peptidic inhibitor) and with two inhibitory caseinopeptides. Numerous publications focus on the inhibition mechanisms of ACE by pharmacological or peptidic inhibitors using conventional enzymatic approaches. However, the resulting values of the inhibitory constants K_i of different molecules depend on the substrate used to perform the study,[28] which complicates data interpretation and the comparison of data resulting from different studies. This drawback can be overcome by eliminating the substrate from the system in direct binding assays. To this end, various methods were used to analyze inhibitor binding to ACE instead of measuring enzymatic inhibition, such as equilibrium dialysis,[34] isothermal titration calorimetry,[13,35] quartz crystal microbalance technique,[14] resonance energy transfer,[12] and fluorescence polarization technique.[36] However, these approaches present a number of disadvantages that limit their application or affect their informative content (lack of sensitivity, high ACE consumption, use of mutated, single-domain or labeled molecules...).[29,37−39]

We present here a comprehensive study that uses a direct label-free approach, SPR-based biosensing, to compare the ACE binding properties of different classes of molecules. In addition, our results show that immobilized ACE can be reused, and this limits the costs of production of the enzyme. In contrast with most of the previous studies, binding measure-

dx.doi.org/10.1021/bi4006144 | *Biochemistry* 2013, 52, 8722−8731

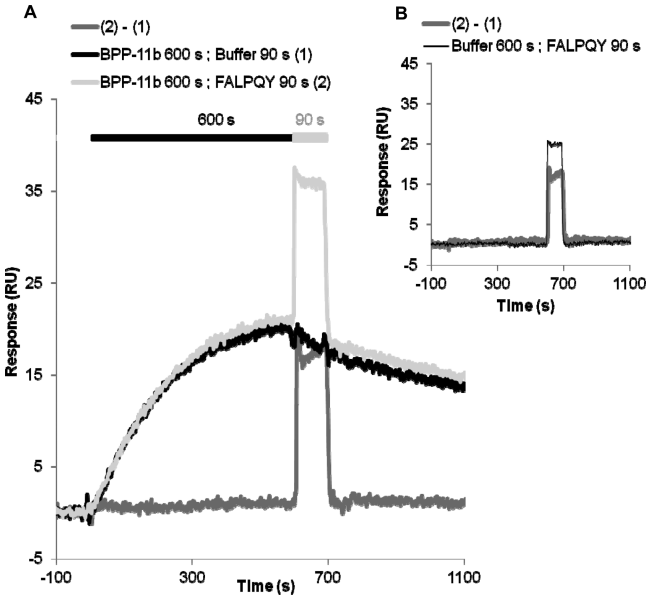

Figure 6. Competition between FALPQY and BPP-11b for binding to immobilized recombinant human somatic ACE (7860 RU). (A) Injection of a 9-nM BPP-11b sample (a concentration that allowed saturating 80% its binding site on ACE) for 600 s followed by a 90-s injection of either buffer (1) or a saturating concentration of FALPQY (30 μM) (2). The signal remaining after subtracting (1) from (2) corresponds to the interaction of FALPQY with the BBP-11b at a concentration saturating 80% its binding site on ACE. (B) Comparison of this remaining (2) − (1) signal with that produced when FALPQY (30 μM) is injected over ACE in the absence of BPP-11b.

ments were performed using the whole two-domain human somatic ACE. The quality of the SPR binding curves combined with their analysis via performing data evaluation approaches enabled a precise description of the ACE−inhibitor binding modes. Moreover, we show that the technology can be employed to determine the binding site(s) of a given ACE inhibitor and differentiate the involvement of the two active sites of ACE in the interaction.

The enzyme inhibition and binding properties of captopril and lisinopril have been previously extensively studied. Enzymatic inhibition assays showed that they bind with different affinities to the two domains of ACE, captopril showing a preference for the amino domain and lisinopril for the carboxyl domain. Nevertheless, results depended on the substrate used in the tests, and the measurements were performed with mutated enzymes or with each of the amino and carboxyl domains separately.[14,17,28,40] Direct binding assays were also performed. Isothermal titration calorimetry studies indicated that captopril bound ACE with a global dissociation constant lower than 10 nM.[13] Moreover, investigation of the binding of [^{3}H]captopril to ACE indicated a global K_D in the nanomolar range. In the case of lisinopril, a global K_D in the nanomolar range was measured using quartz crystal microbalance[14] and in the 20-nM range using fluorescence polarization.[36]

The SPR analysis of the whole two-domain ACE binding to the pharmacological inhibitors, combined with the kinetic distribution analysis of the binding curves, clearly indicated the existence of two interactions with similar on-rate constants and different off-rate constants (Figure 3). The two K_D's differed by a factor 10−20 in the case of captopril, and >30 in the case of lisinopril. Considering the earlier findings that captopril and lisinopril preferentially bind to the amino and carboxyl domains of ACE, respectively,[17,28,40] we can speculate that captopril binds the amino and carboxyl domains with K_D's around 0.2 and 3 nM, respectively, and that lisinopril binds these domains with K_D's > 8 and around 0.2 nM, respectively. The fast formation of ACE−captopril complex and its slow dissociation are consistent with the clinical efficiency of captopril in the treatment of hypertension.[7]

The interaction of the snake venom peptide BPP-11b with the enzyme was also investigated by SPR, indicating a nanomolar affinity and a corrected stoichiometry of 1. This interaction probably corresponded to BPP-11b binding to the carboxyl domain active site, as Cotton et al. have found that BPP-11b was 266-fold more selective for the carboxyl domain of ACE than for the amino domain (apparent K_i = 30 and 8000 nM, respectively).[18]

Besides these strong inhibitors, many peptides able to inhibit ACE activity *in vitro* have been isolated from food protein sources, notably milk, but their mechanism of binding to ACE is still misunderstood. Tryptic digestion of α_{s2}-casein leads to produce ACE-inhibitory peptides among which FALPQYLK and FALPQY are the most efficient with the same IC_{50} of 4.3 μM, a value lower than IC_{50} of most of the inhibitory caseinopeptides.[10] The inhibitory potency of FALPQYLK could not be attributed to the generation of FALPQY by ACE as only 2% of FALPQYLK was hydrolyzed into FALPQY by ACE in the presence and the absence of the synthetic substrate HHL.[10] Therefore, these peptides were chosen to compare their mode of binding to human ACE with that of the stronger inhibitors (pharmacological inhibitors, BPP-11b). A fast dissociation immediately after stopping the injection into the microfluidic system was observed, resulting in a much weaker affinity compared to the pharmacological inhibitors captopril and lisinopril, with similar K_D's values of 3.1 and 3.7 μM respectively. This confirmed that the two carboxyl-terminal residues LK did not have any role in determining the affinity of these peptides to ACE.[10] Moreover, the corrected binding stoichiometries indicated that the α_{s2}-caseinopeptides FALPQYLK and FALPQY bound to two sites on ACE. The ability of captopril and BPP-11b to fully and partly, respectively, block FALPQY binding to ACE in a SPR competition assay indicated that the α_{s2}-caseinopeptide recognized the active site regions on both amino and carboxyl domains of ACE. The SPR study thus demonstrated that (i) the caseinopeptides FALPQYLK and FALPQY, unlike the other inhibitors studied in this work, form an unstable complex with ACE, (ii) the two caseinopeptide molecules are able to interact with one enzyme molecule, and (iii) the peptide binding sites and ACE active sites overlap.

We show here that SPR analysis is a complementary tool to enzymological investigations, as it represents an efficient means to determine the $t_{1/2}$ of ACE−inhibitor complex, its binding stoichiometry, and the location of the binding site(s) of the inhibitor on ACE. The technology is suitable to predict, in a first step, if a molecule interacting with ACE *in vitro* possesses some potentiality to be antihypertensive *in vivo* before carrying out investigations on its bioavailability and its capability of lowering the level of blood pressure *in vivo*, or displays any other biological activity related to its selective interaction with the amino domain.[41] Indeed, whereas pharmacological inhibitors such as enalapril, lisinopril, and fosinopril are, like captopril, able to inhibit both amino and carboxyl domains of ACE,[28] their chronic use in the treatment of hypertension may

dx.doi.org/10.1021/bi4006144 | *Biochemistry* 2013, 52, 8722−8731

lead to some undesirable effects which have been attributed to the accumulation of bradykinin after full inhibition of ACE.[5] Therefore, several studies focus on molecules able to inhibit ACE in a selective way. According to Georgiadis et al., the selective inhibition of ACE carboxyl domain could lead to a reduction of blood pressure, without altering bradykinin degradation by the amino domain active site, and could thus reduce side effects.[42] On the other hand, selective inhibition of the amino domain could prevent cardiac and renal fibrosis,[43] as the administration of the antifibrotic acetyl-SDKP to Sprague–Dawley rats lead to minimize collagen deposition and cell proliferation in the heart and the kidney.[44,45] With this regard, the approach presented here was shown to be a quick and efficient mean to assess the binding domain of a given molecule and the selection of those possessing the desired properties.

In conclusion, we were able to characterize the ACE–inhibitor binding mode using the SPR technology, combined with the regression or kinetic distribution analysis of the binding curves. These approaches represent an efficient means to select inhibitors that form stable complexes with ACE, which is a prerequisite for an efficient action *in vivo*, and to investigate their selectivity toward the amino or the carboxyl domain of ACE. They could thus be employed, in a first step, to select promising inhibitors, prior to more time-consuming *in vivo* experiments.

■ ASSOCIATED CONTENT

Supporting Information

Kinetic distribution analysis of the ACE–captopril, ACE–lisinopril, and ACE–BPP-11b curves evaluated with the Interaction Map software.

This material is available free of charge *via* the Internet at http://pubs.acs.org

■ AUTHOR INFORMATION

Corresponding Author

*E-mail: celine.cakir-kiefer@univ-lorraine.fr; phone: +33 383684269; fax: +33 383684274.

Notes

The authors declare no competing financial interest.

■ ACKNOWLEDGMENTS

The authors gratefully acknowledge Prof. François Alhenc-Gelas from the Institut National de la Santé et de la Recherche Médicale (INSERM, Paris, France) for the gift of CHO-ACE cell line. The authors also thank Prof. Marie Trabalon and Mrs. Christiane Tankosik from the Équipe de Physiologie du Comportement (Université de Lorraine, Nancy, France) and Ms. Alyah Kosayyer (UR AFPA) for experiments and cell culture technical help, and Mr. Cédric Paris from the Plateau Analyse Structurale et Métabolomique (Université de Lorraine) for mass spectrometry analysis. D.A. and G.Z.-L. acknowledge support from the Centre National de la Recherche Scientifique (CNRS) and Université de Strasbourg (UdS). The authors thank Mr. Karl Andersson (Ridgeview Diagnostics AB) for Interaction Map calculation and for constructive discussions. F. Z. is sincerely grateful to Mr. Tom Morton (BioLogic Software, Campbell, Australia) for the gift of Scrubber 2.0c software and for his valuable assistance.

■ ABBREVIATIONS

ACE, angiotensin I-converting enzyme; BPPs, bradykinin potentiating peptides; CHO-ACE, Chinese hamster ovary cell line transfected with a full-length cDNA encoding human somatic angiotensin I-converting enzyme; FC, flow cell; HHL, hippuryl-L-His-L-Leu; HBS, Hepes buffered saline; MCK, multicycle kinetics; *n*, stoichiometry; RU, resonance unit; SCK, single cycle kinetics; SPR, surface plasmon resonance

■ REFERENCES

(1) Soubrier, F., Alhenc-Gelas, F., Hubert, C., Allegrini, J., John, M., Tregear, G., and Corvol, P. (1988) Two putative active centers in human angiotensin I-converting enzyme revealed by molecular cloning. *Proc. Natl. Acad. Sci. U.S.A. 85*, 9386–9390.

(2) Ferreira, S. H., Bartelt, D. C., and Greene, L. J. (1970) Isolation of bradykinin-potentiating peptides from *Bothrops jararaca* venom. *Biochemistry 9*, 2583–2593.

(3) Hayashi, M. A. F., Murbach, A. F., Ianzer, D., Portaro, F. C. V., Prezoto, B. C., Fernandes, B. L., Silveira, P. F., Silva, C. A., Pires, R. S., Britto, L. R., Dive, V., and Camargo, A. C. (2003) The C-type natriuretic peptide precursor of snake brain contains highly specific inhibitors of the angiotensin-converting enzyme. *J. Neurochem. 85*, 969–977.

(4) Rioli, V., Prezoto, B. C., Konno, K., Melo, R. L., Klitzke, C. F., Ferro, E. S., Ferreira-Lopes, M., Camargo, A. C., and Portaro, F. C. (2008) A novel bradykinin potentiating peptide isolated from *Bothrops jararacussu* venom using catallytically inactive oligopeptidase EP24.15. *FEBS J. 275*, 2442–2454.

(5) Camargo, A. C. M., Ianzer, D., Guerreiro, J. R., and Serrano, S. M. T. (2012) Bradykinin-potentiating peptides: Beyond captopril. *Toxicon 59*, 516–523.

(6) Cushman, D. W., Cheung, H. S., Sabo, E. F., and Ondetti, M. A. (1977) Design of potent competitive inhibitors of angiotensin-converting enzyme. Carboxyalkanoyl and mercaptoalkanoyl amino acids. *Biochemistry 16*, 5484–5491.

(7) Brown, N. J., and Vaughan, D. E. (1998) Angiotensin-converting enzyme inhibitors. *Circulation 97*, 1411–1420.

(8) FitzGerald, R. J., Murray, B. A., and Walsh, D. J. (2004) Hypotensive peptides from milk proteins. *J. Nutr. 134*, 980S–988S.

(9) Cao, W., Zhang, C., Ji, H., and Hao, J. (2012) Optimization of peptic hydrolysis parameters for the production of angiotensin I-converting enzyme inhibitory hydrolysate from *Acetes chinensis* through Plackett-Burman and response surface methodological approaches. *J. Sci. Food Agric. 92*, 42–48.

(10) Tauzin, J., Miclo, L., and Gaillard, J. L. (2002) Angiotensin-I-converting enzyme inhibitory peptides from tryptic hydrolysate of bovine α_{s2}-casein. *FEBS Lett. 531*, 369–374.

(11) Cushman, D. W., and Cheung, H. S. (1971) Spectrophotometric assay and properties of the angiotensin-converting enzyme of rabbit lung. *Biochem. Pharmacol. 20*, 1637–1648.

(12) Sabatini, R. A., Bersanetti, P. A., Farias, S. L., Juliano, L., Juliano, M. A., Casarini, D. E., Carmona, A. K., Paiva, A. C., and Pesquero, J. B. (2007) Determination of angiotensin I-converting enzyme activity in cell culture using fluorescence resonance energy transfer peptides. *Anal. Biochem. 363*, 255–262.

(13) Ortiz-Salmerón, E., Barón, C., and García-Fuentes, L. (1998) Enthalpy of captopril-angiotensin I-converting enzyme binding. *FEBS Lett. 435*, 219–224.

(14) Su, Z., Chen, L., Liu, Y., He, X., Zhou, Y., Xie, Q., and Yao, S. (2011) 35 MHz quartz crystal microbalance and surface plasmon resonance studies on the binding of angiotensin converting enzyme with lisinopril. *Biosens. Bioelectron. 26*, 3240–3245.

(15) Papalia, G. A., Baer, M., Luehrsen, K., Nordin, H., Flynn, P., and Myszka, D. G. (2006) High-resolution characterization of antibody fragment/antigen interactions using Biacore T100. *Anal. Biochem. 359*, 112–119.

(16) Takahashi, S., Ono, H., Gotoh, T., Yoshizawa-Kumagaye, K., and Sugiyama, T. (2011) Novel internally quenched fluorogenic

substrates for angiotensin I-converting enzyme and carboxypeptidase Y. *Biomed. Res. 32*, 407−411.
(17) Wei, L., Clauser, E., Alhenc-Gelas, F., and Corvol, P. (1992) The two homologous domains of human angiotensin I-converting enzyme interact differently with competitive inhibitors. *J. Biol. Chem. 267*, 13398−13405.
(18) Cotton, J., Hayashi, M. A. F., Cuniasse, P., Vazeux, G., Ianzer, D., De Camargo, A. C. M., and Dive, V. (2002) Selective inhibition of the C-domain of angiotensin I converting enzyme by bradykinin potentiating peptides. *Biochemistry 41*, 6065−6071.
(19) Wei, L., Alhenc-Gelas, F., Soubrier, F., Michaud, A., Corvol, P., and Clauser, E. (1991) Expression and characterization of recombinant human angiotensin I-converting enzyme. Evidence for a C-terminal transmembrane anchor and for a proteolytic processing of the secreted recombinant and plasma enzymes. *J. Biol. Chem. 266*, 5540−5546.
(20) Bull, H. G., Thornberry, N. A., and Cordes, E. H. (1985) Purification of angiotensin-converting enzyme from rabbit lung and human plasma by affinity chromatography. *J. Biol. Chem. 260*, 2963−2972.
(21) Laemmli, U. K. (1970) Cleavage of structural proteins during the assembly of the head of bacteriophage T4. *Nature 227*, 680−685.
(22) Zidane, F., Matéos, A., Cakir-Kiefer, C., Miclo, L., Rahuel-Clermont, S., Girardet, J. M., and Corbier, C. (2012) Binding of divalent metal ions to 1−25 β-caseinophosphopeptide: an isothermal titration calorimetry study. *Food Chem. 132*, 391−398.
(23) Bradford, M. M. (1976) A rapid and sensitive method for the quantification of microgram quantities of protein utilizing the principle of protein-dye-binding. *Anal. Biochem. 72*, 248−254.
(24) Frister, H., Meisel, H., and Schlimme, E. (1988) OPA method modified by use of *N*,*N*-dimethyl-2-mercaptoethylammonium chloride as thiol component. *Fresenius Z. Anal. Chem. 330*, 631−633.
(25) Miclo, L., Perrin, E., Driou, A., Papadopoulos, V., Boujrad, N., Vanderesse, R., Boudier, J. F., Desor, D., Linden, G., and Gaillard, J. L. (2001) Characterization of α-casozepine, a tryptic peptide from bovine α_{s1}-casein with benzodiazepine-like activity. *FASEB J. 15*, 1780−1782.
(26) Lanzillo, J. J., Stevens, J., Dasarathy, Y., Yotsumoto, H., and Fanburg, B. L. (1985) Angiotensin-converting enzyme from human tissues. Physicochemical, catalytic, and immunological properties. *J. Biol. Chem. 260*, 14938−14944.
(27) Nishimura, K., Hiwada, K., Ueda, E., and Kokubu, T. (1976) Solubilization of angiotensin I-coverting enzyme from rabbit lung using trypsin treatment. *Biochim. Biophys. Acta 452*, 144−150.
(28) Marquart, J. A. (2012) *Surface Plasmon Resonance and Biomolecular Interaction Analysis: Theory and Practice* (Marquart, J. A., Eds.), 3rd ed., pp 1−191.
(29) Michaud, A., Williams, T. A., Chauvet, M. T., and Corvol, P. (1997) Substrate dependence of angiotensin I-converting enzyme inhibition: captopril displays a partial selectivity for inhibition of *N*-acetyl-seryl-aspartyl-lysyl-proline hydrolysis compared with that of angiotensin I. *Mol. Pharmacol. 51*, 1070−1076.
(30) Svitel, J., Balbo, A., Mariuzza, R. A., Gonzales, N. R., and Schuck, P. (2003) Combined affinity andrate constant distributions of ligand populations from experimental surface binding kinetics and equilibria. *Biophys. J. 84*, 4062−4077.
(31) Svitel, J., Boukari, H., Van Ryk, D., Willson, R. C., and Schuck, P. (2007) Probing the functional heterogeneity of surface binding sites by analysis of experimental binding traces and the effect of mass transport limitation. *Biophys. J. 92*, 1742−1758.
(32) Björkelund, H., Gedda, L., Barta, P., Malmqvist, M., and Andersson, K. (2011) Gefitinib induces epidermal growth factor receptor dimers which alters the interaction characteristics with ^{125}I-EGF. *PLoS One 6*, e24739.
(33) Altschuh, D., Björkelund, H., Strandgård, J., Choulier, L., Malmqvist, M., and Andersson, K. (2012) Deciphering complex protein interaction kinetics using Interaction Map. *Biochem. Biophys. Res. Commun. 428*, 74−79.
(34) Bree, F., Nguyen, P., Urien, S., Resplandy, G., and Tillement, J. P. (1992) Specific and high affinity binding of perindoprilat, but not of perindopril to blood ACE. *Int. J. Clin. Pharmacol. Ther. Toxicol. 30*, 325−330.
(35) Andújar-Sánchez, M., Cámara-Artigas, A., and Jara-Pérez, V. (2004) A calorimetric study of the binding of lisinopril, enalaprilat and captopril to angiotensin-converting enzyme. *Biophys. Chem. 111*, 183−189.
(36) Voronov, S. V., Binevski, P. V., Eremin, S. A., and Kost, O. A. (2001) Fluorescence polarization studies of different forms of angiotensin-converting enzyme. *Biochemistry 66*, 788−794.
(37) Shapiro, R., and Riordan, J. F. (1984) Inhibition of angiotensin converting enzyme: dependence of chloride. *Biochemistry 23*, 5234−5240.
(38) Strittmatter, S. M., and Snyder, S. H. (1986) Characterization of angiotensin converting enzyme by [3H]captopril binding. *Mol. Pharmacol. 29*, 142−148.
(39) Reynolds, C. H. (1984) Kinetics of inhibition of angiotensin converting enzyme by captopril and by enalapril diacid. *Biochem. Pharmacol. 33*, 1273−1276.
(40) Tzakos, A. G., and Gerothanassis, I. P. (2005) Domain-selective ligand-binding modes and atomic level pharmacophore refinement in angiotensin I converting enzyme (ACE) inhibitors. *ChemBiochem 6*, 1089−1103.
(41) Rousseau, A., Michaud, A., Chauvet, M. T., Lenfant, M., and Corvol, P. (1995) The hemoregulatory peptide *N*-acetyl-Ser-Asp-Lys-Pro is a natural and specific substrate of the N-terminal active site of human angiotensin-converting enzyme. *J. Biol. Chem. 270*, 3656−3661.
(42) Georgiadis, D., Beau, F., Czarny, B., Cotton, J., Yiotakis, A., and Dive, V. (2003) Roles of the two active sites of somatic angiotensin-converting enzyme in the cleavage of angiotensin I and bradykinin: insights from selective inhibitors. *Circ. Res. 93*, 148−154.
(43) Kroger, W. L., Douglas, R. G., O'Neill, H. G., Dive, V., and Sturrock, E. D. (2009) Investigating the domain specificity of phosphinic inhibitors RXPA380 and RXP407 in angiotensin-converting enzyme. *Biochemistry 48*, 8405−8412.
(44) Peng, H., Carretero, O. A., Raij, L., Yang, F., Kapke, A., and Rhaleb, N. E. (2001) Antifibrotic effects of *N*-acetyl-seryl-aspartyl-Lysyl-proline on the heart and kidney in aldosterone-salt hypertensive rats. *Hypertension 37*, 794−800.
(45) Cavasin, M. A., Liao, T. D., Yang, X. P., Yang, J. J., and Carretero, O. A. (2007) Decreased endogenous levels of Ac-SDKP promote organ fibrosis. *Hypertension 50*, 130−136.